On the fractal dimension and lacunarity for a sample of δScuti

Francisco Paz-Chinchón*
fpazch@illinois.edu

December 24, 2016

Abstract

Fractal dimension and lacunarity were calculated for a set of light curves belonging to δScuti stars. Box counting was the selected method, alongside with a parallel lacunarity calculation. For the fractal dimension, we get results coherent with correlated data points, with low complexity and persistent behavior. For the lacunarity, small box size shows a higher similarity when compared to the larger. In conclusion, for the smaller scales here analyzed, time series behaves persistent, correlated, and are similar between blocks.

1 Brief method review

Fractal dimension (hereafter D) can be assessed through different methods, from which one of the most widely used is the box-counting algorithm. Basically, it consists in divide the object in boxes of same size and then count how many of them has mass different from zero (namely, boxes harboring at least one data point). The calculation is repeated for different box sizes (hereafter r), then a plot is created on the log-log space for the inverse of the box size (sometimes called magnification) against the number of non-zero mass boxes (hereafter $\mathcal{N}(r)$). Therefore, fractal dimension is defined as the slope of the first order polynomial fit, for the generated set of points,

$$\mathcal{N}(r) = \mathcal{A}\, r^{-D} \tag{1}$$

$$\log_{10} \mathcal{N}(r) = \log_{10} \mathcal{A} + D \log_{10} \left(\frac{1}{r}\right) \tag{2}$$

where $\mathcal{N}(r)$ is the number of non-empty boxes, for a given r, $\mathcal{A}(r)$ is the lacunarity, and D is the fractal dimension. The fact of showing a power-law characteristic is an indicative of self-similarity.

Given its simplicity, box-counting is a good method for assess the fractal dimension of the objects, as a first diagnosis of the non-linear behavior.

Besides the value of D, calculation of lacunarity also give us important information. Lacunarity can be conceived as the deviation of a fractal from translational invariance. As translational invariance is strongly dependent on the scale (or in our case, box size), thus lacunarity is here considered as a scale-dependent measure of the *texture* of an object [Plotnick et al., 1996]. Note that this is not an exclusive property of fractal objects.

Additionally to the calculation of the overall $\mathcal{A}$ in Eq. 2, we employed the Allain and Cloitre [1991] method (the gliding-box algorithm) for calculating the lacunarity at each box size, following the proposed recipe on which the value is obtained through the first and second distribution moments of the probability function (hereafter $Q(\cdot)$) for a sample of box masses (hereafter s, number of occupied sites within the boxes), given a box size,

$$\mathcal{A}(r) = \frac{Z_Q^{(2)}(r)}{\left(Z_Q^{(1)}(r)\right)^2} \tag{3}$$

$$Z_Q^{(q)}(r) = \sum_s s^q Q(s, r) \tag{4}$$

*National Center for Supercomputing Applications, NCSA. University of Illinois.

where $Z_Q^{(1)}(r)$ and $Z_Q^{(2)}(r)$ can be defined in terms of variance ($s_s^2(r)$) and mean ($\langle s(r) \rangle$) [Plotnick et al., 1996],

$$Z_Q^{(1)}(r) = \langle s(r) \rangle \quad , \quad Z_Q^{(2)}(r) = s_s^2(r) + \langle s(r) \rangle^2 \tag{5}$$

As stated by Allain and Cloitre [1991], in the case of a translationally invariant object, $Q(s, r)$ is a Dirac function, given as result lacunarity with unity value, $\forall\, r$.

2 Code

For all the light curves, no any assumption was made (even the sampling rate was calculated from scratch). For the fractal dimension calculation we iterated over increasing box sizes, where the minimal box was obtained by calculating sampling rate over a representative subset of points, drawn from a Normal random selection. Thus the minimal box size was set as the sampling rate, and then the size was increased by multiplying this value by the next integer[1]. For each light curve, 1 000 box sizes were input to the calculation, covering from ∼32 s to ∼ 32 000 s (∼8.89 h).

To deal with boundaries, data were replicated through symmetric reflection: $x_2, x_1 | x_0, x_1, \ldots, x_{n-1}, x_n | x_{n-1}, x_{n-2}$

An mimic of the counting code (developed in Python 2.7) is shown below to illustrate part of the algorithm,

```
low_limit = np.fromfunction(lambda i: (i*box_size),(N_r,),dtype=np.float)
low_limit += pad_data['time'][0]
counter = 0L
for it in np.nditer(low_limit):
    cond = np.where(np.logical_and(pad_data['time'] >= it,pad_data['time'] < (it+box_size)))
    if (pad_data[cond].shape[0]  > 0):
        counter += 1
```

It is important to note that in this implementation, boxes are vertical sections covering all the range of fluxes, for a given range in time. No measurements were made implementing a square-box grid.

For the linear fits (Eq. 2), two competing methods were employed: non-linear least-squares (`scipy`) and ordinary least-squares (`statsmodels`). Even when both agree within the error bars, the ordinary least-squares approach was selected because of the more realistic values of the errors, for in fractal dimension and lacunarity. Results of the fits, jointly with the logarithmic likelihood of the adjustment are shown in Table 1.

For the calculation of lacunarity at each box size, we employed Eqs. 3-5, at each of the 1 000 different box sizes.

3 Results

First of all, all plots (Figs. 1-6) are labeled by its filename, and posses 3 parts. Upper left panel shows the log-log plot of the inverse of box size versus the number of non-empty boxes, with data points in blue and the linear fit in red. Lower left panel shows the magnification versus the overall lacunarity (from Eq. 2) as orange dashed horizontal line, while on green are shown the values for inverse box size versus the scale dependent lacunarity (from Eq. 3). Right panel shows a window of the light curve, equivalent to the ceiling value of the inverse of the sampling rate (window of one day). Axes are time[2]in calendar units versus the flux normalized by its mean.

Table 1 exhibits the results for the ordinary least-squares fits for the log-log plots. On the first column the ID were taken from the filenames, second column shows the value of the fractal dimension, third column shows the logarithmic value of the overall lacunarity, and fourth column shows the log-likelihood value of the fit.

Even when this is a simple estimation, which can be refined based on which scale it is desired to target, results are indicatives of some clear outputs:

- behavior of the analyzed time series is highly monofractal,
- the system is persistent: the level of correlation and predictability in small scales (given our box sizes) is strong,

[1] As we were interested in the small scale effects, this was a reasonable assumption.
[2] Julian Date was assumed for time axis, with a the CoRoT time delay of 2451545 JD.

- at the analyzed scales, the systems shows a low complexity,
- at the analyzed scales, the overall behavior is smooth.

As the first item points, and Figs. 1-6 exhibits, all the time series can be characterized by a single power-law relation over the entire range of r. This is an indicative of the monofractal nature over the range of box sizes, which also shows the low level of complexity of these objects.

As our analysis was centered on small scales (wider box size is slightly smaller than 9 h), and the fractal dimension is close to 1, we can infer a high level of correlation between points. The high correlation also give us the chance of predict the behavior of adjacent data points, based on a *small* vicinity (referring to our available r). It is remarkable the small errors for all the fitted slope values, as seen on Table 1.

Smooth behavior can be inferred with a more careful interpretation: the overall smoothness can be hiding some local sharpness. Must be noticed that this calculation of the fractal dimension shows a monofractal behavior with $D \sim 1$, but it is recommendable to perform a more dedicated analysis over the scales of special interest.

Regarding the overall lacunarity calculations, a higher dispersion is observed in values. Whereas they are not meaningful by its own, but when compared among others: that is the motivation to perform the scale dependent measure ($\mathcal{A}(r)$).

For $\mathcal{A}(r)$, higher values means a lower translational invariance whereas lower values shows a higher self similarity when blocks of data are compared. It is expected that at higher box sizes, $\mathcal{A}(r)$ must assume higher values, reflecting that the object at this scale shows a lower similarity between blocks when compared with smaller scale. Its is noticeable from the plots with filenames ending in "a" and "l" a rapid decrease in the value, indicating translational invariance is a feature for these light curves at small scales. Namely, when $\mathcal{A}(r) \sim 1$.

In the other hand, light curves whose filenames ends in "g" shows a similar double decay: first from the higher r up to $r \sim 0.0687$ d ($r^{-1} \sim 14.55$) and then a lower decay up to the higher magnification (maybe it would be worthy to analyze this change in slope). The last decay did not reach the lower values exhibited by the first set of data ("a" and "l"). Special attention deserves HD41641g (Fig. 4), showing a linear decay without the inflection point at $r \sim 0.0687$ d, but further interpretation is beyond the scope of the available results.

Results for D and $\mathcal{A}(r)$ for each r are given as `numpy` record arrays (structured arrays), in attachment.

References

C. Allain and M. Cloitre. Characterizing the lacunarity of random and deterministic fractal sets. *Physical Review A*, 44(6), 1991.

Roy E. Plotnick, Robert H. Gardner, William W. Hargrove, Karen Prestegaard, and Amrtin Pelmutter. Lacunarity analysis: A general technique for the analysis of spatial patterns. *Physical Review E*, 53(5), 1996.

ID	D	$\log_{10}\mathcal{A}$	$\log_{10}\mathcal{L}$
GSC00144-03031a	0.99820 ±0.00004	1.90142 ±0.00004	6096
GSC00144-03031g	0.98964 ±0.00015	1.90645 ±0.00015	4683
GSC00144-03031l	0.99820 ±0.00004	1.90143 ±0.00004	6096
HD170699a	0.99841 ±0.00003	1.95348 ±0.00003	6210
HD170699g	0.99204 ±0.00019	1.95790 ±0.00019	4482
HD170699l	0.99841 ±0.00003	1.95348 ±0.00003	6209
HD172189a	0.99904 ±0.00002	2.17486 ±0.00002	6720
HD172189g	0.99312 ±0.00018	2.17879 ±0.00018	4494
HD172189l	0.99904 ±0.00002	2.17487 ±0.00002	6726
HD174532a	0.99463 ±0.00012	1.42813 ±0.00012	5002
HD174532g	0.98255 ±0.00015	1.43551 ±0.00015	4647
HD174532l	0.99462 ±0.00012	1.42814 ±0.00012	5005
HD174589a	0.99462 ±0.00012	1.42698 ±0.00012	4997
HD174589g	0.98263 ±0.00016	1.43421 ±0.00016	4632
HD174589l	0.99462 ±0.00012	1.42698 ±0.00012	4997
HD174936a	0.99484 ±0.00011	1.44323 ±0.00011	5040
HD174936g	0.98867 ±0.00019	1.44807 ±0.00019	4474
HD174936l	0.99483 ±0.00011	1.44334 ±0.00011	5035
HD174966a	0.99482 ±0.00011	1.44339 ±0.00011	5038
HD174966g	0.98922 ±0.00018	1.44774 ±0.00018	4539
HD174966l	0.99482 ±0.00011	1.44339 ±0.00011	5038
HD181555a	0.99909 ±0.00002	2.19647 ±0.00002	6796
HD181555g	0.99337 ±0.00021	2.20059 ±0.00021	4388
HD181555l	0.99910 ±0.00002	2.19647 ±0.00002	6788
HD41641a	0.99849 ±0.00003	1.97769 ±0.00003	6269
HD41641g	0.98868 ±0.00016	1.95344 ±0.00016	4600
HD41641l	0.99849 ±0.00003	1.97769 ±0.00003	6269
HD48784a	0.99444 ±0.00012	1.41274 ±0.00012	4970
HD48784g	0.98787 ±0.00019	1.41769 ±0.00019	4490
HD48784l	0.99444 ±0.00012	1.41274 ±0.00012	4970
HD49434a	0.99896 ±0.00002	2.13816 ±0.00002	6648
HD49434g	0.98935 ±0.00020	2.14353 ±0.00020	4389
HD49434l	0.99896 ±0.00002	2.13816 ±0.00002	6646
HD50844a	0.99753 ±0.00005	1.76548 ±0.00005	5786
HD50844g	0.99141 ±0.00020	1.77001 ±0.00020	4411
HD50844l	0.99754 ±0.00005	1.76548 ±0.00005	5779
HD50870a	0.99875 ±0.00003	2.06062 ±0.00003	6464
HD50870g	0.99331 ±0.00018	2.06441 ±0.00018	4533
HD50870l	0.99875 ±0.00003	2.06062 ±0.00003	6464
HD51359a	0.99879 ±0.00003	2.07178 ±0.00003	6502
HD51359g	0.99288 ±0.00019	2.07598 ±0.00019	4452
HD51359l	0.99879 ±0.00003	2.07178 ±0.00003	6502
HD51722a	0.99878 ±0.00003	2.07165 ±0.00003	6471
HD51722g	0.99285 ±0.00019	2.07585 ±0.00019	4488
HD51722l	0.99878 ±0.00003	2.07165 ±0.00003	6471

Table 1: Table with the results of the fractal dimension and logarithmic lacunarity least-squares fit. Last column exposes the logarithmic likelihood of the fit. A word of caution about the log-likelihood values here exhibited: their values are extremely high because of the goodness of fit, and must be used for comparison only.

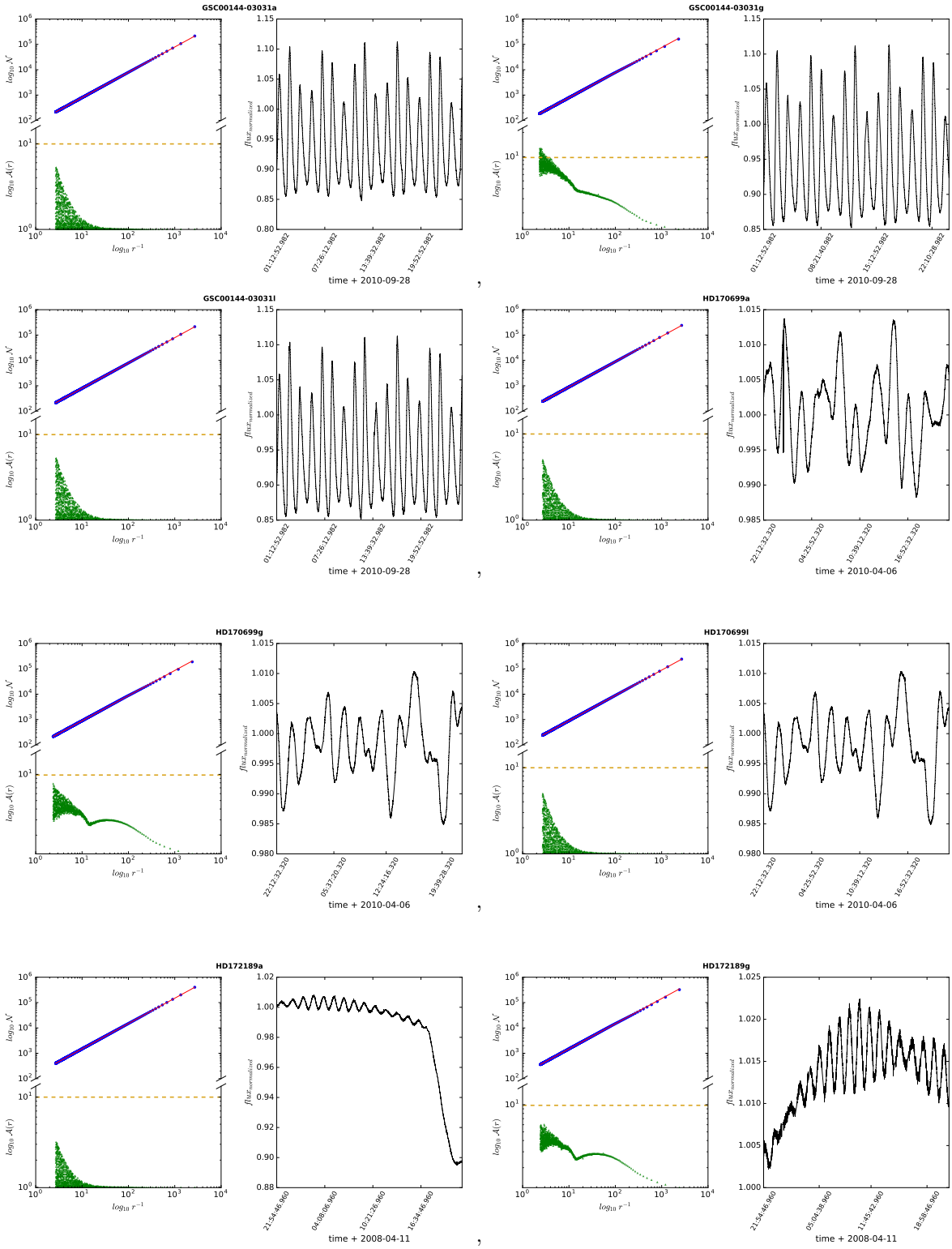

Figure 1: Set 1.

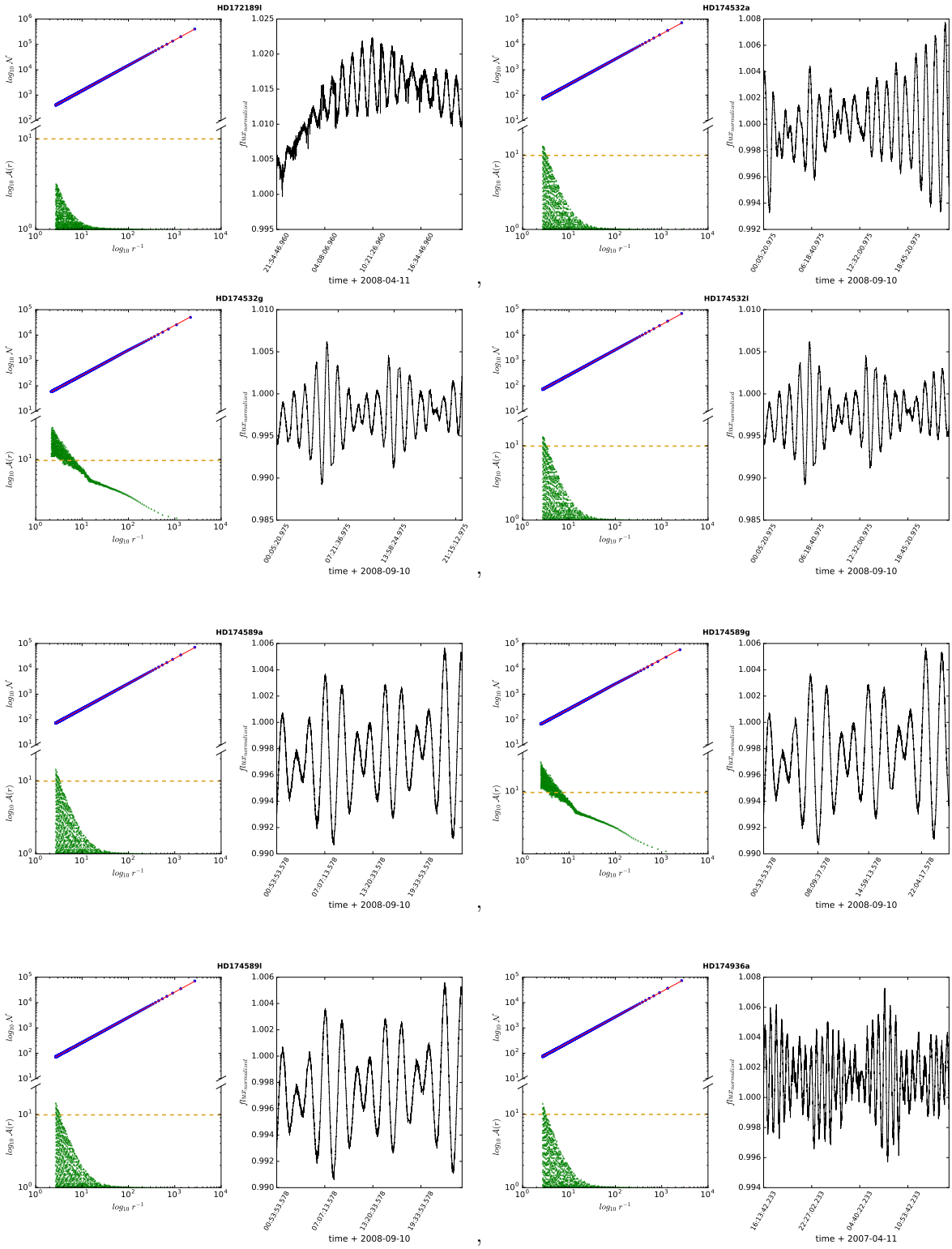

Figure 2: Set 2.

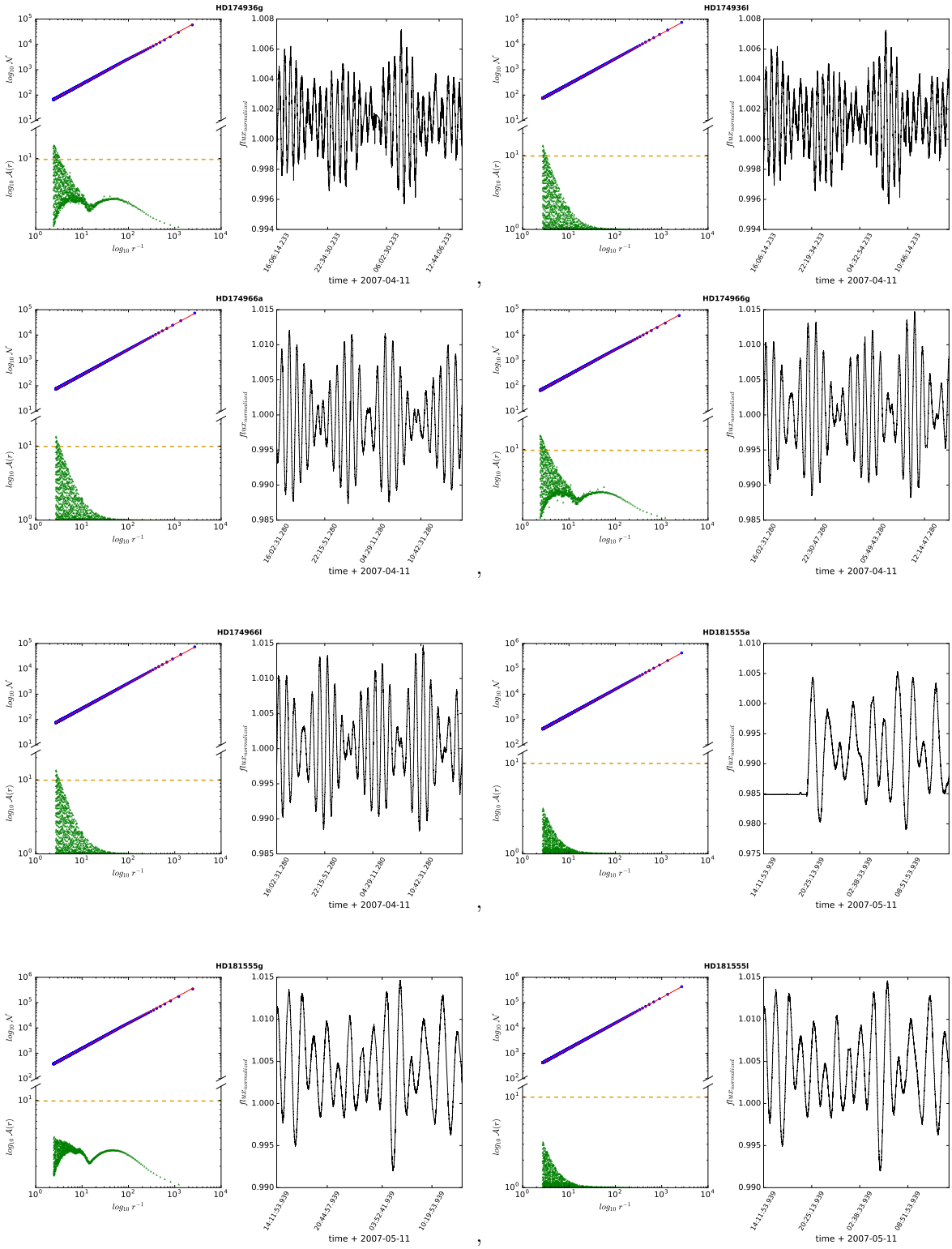

Figure 3: Set 3.

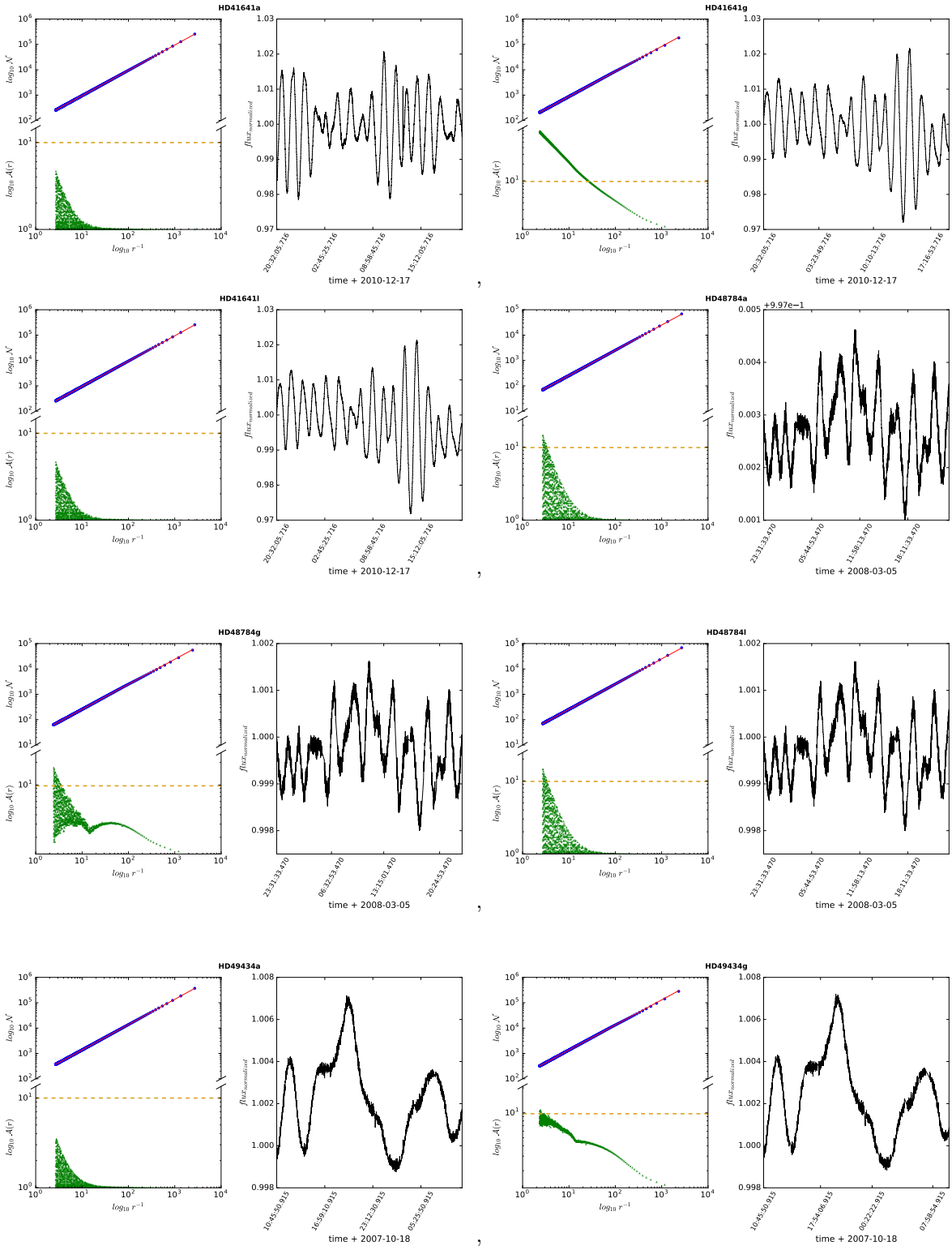

Figure 4: Set 4.

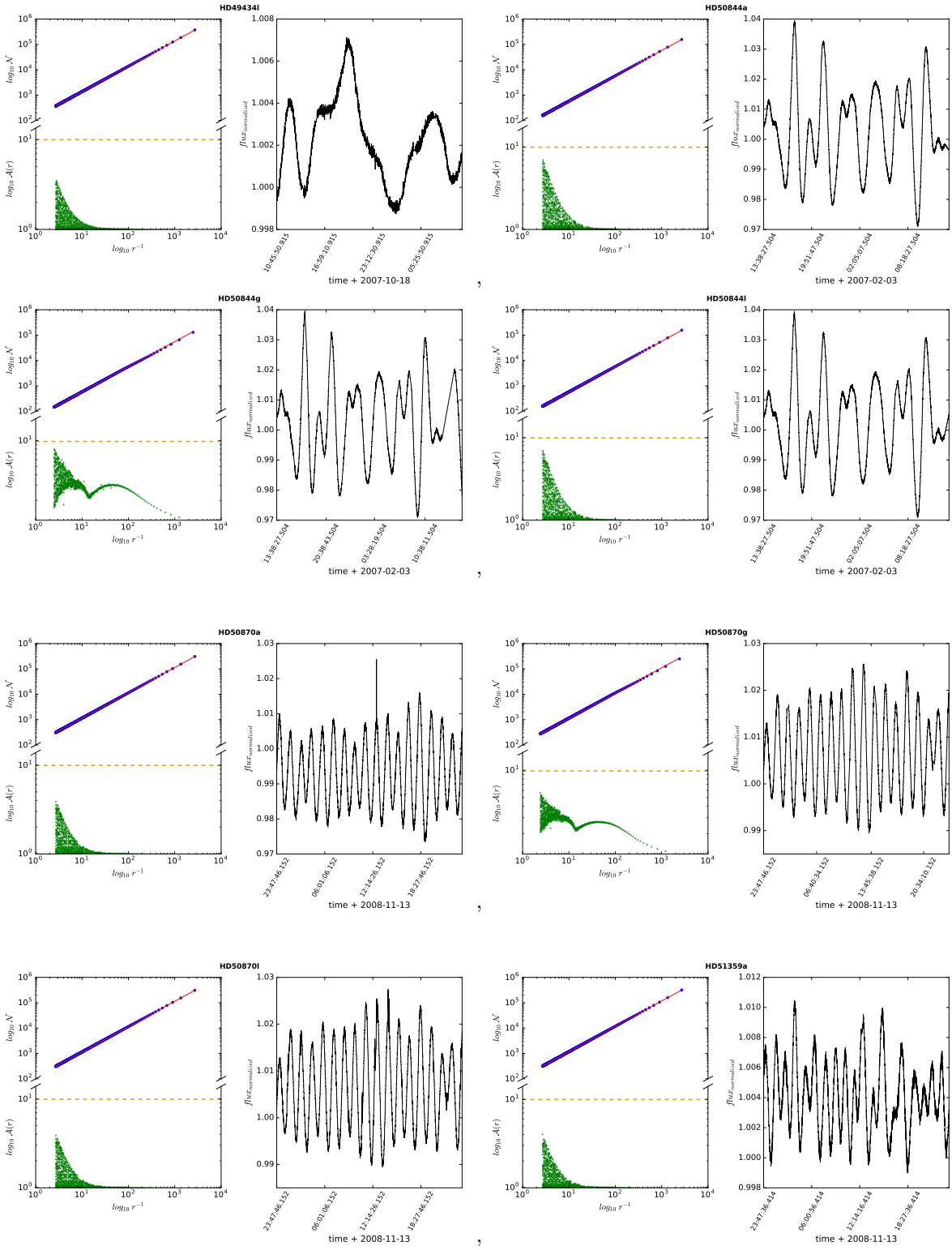

Figure 5: Set 5.

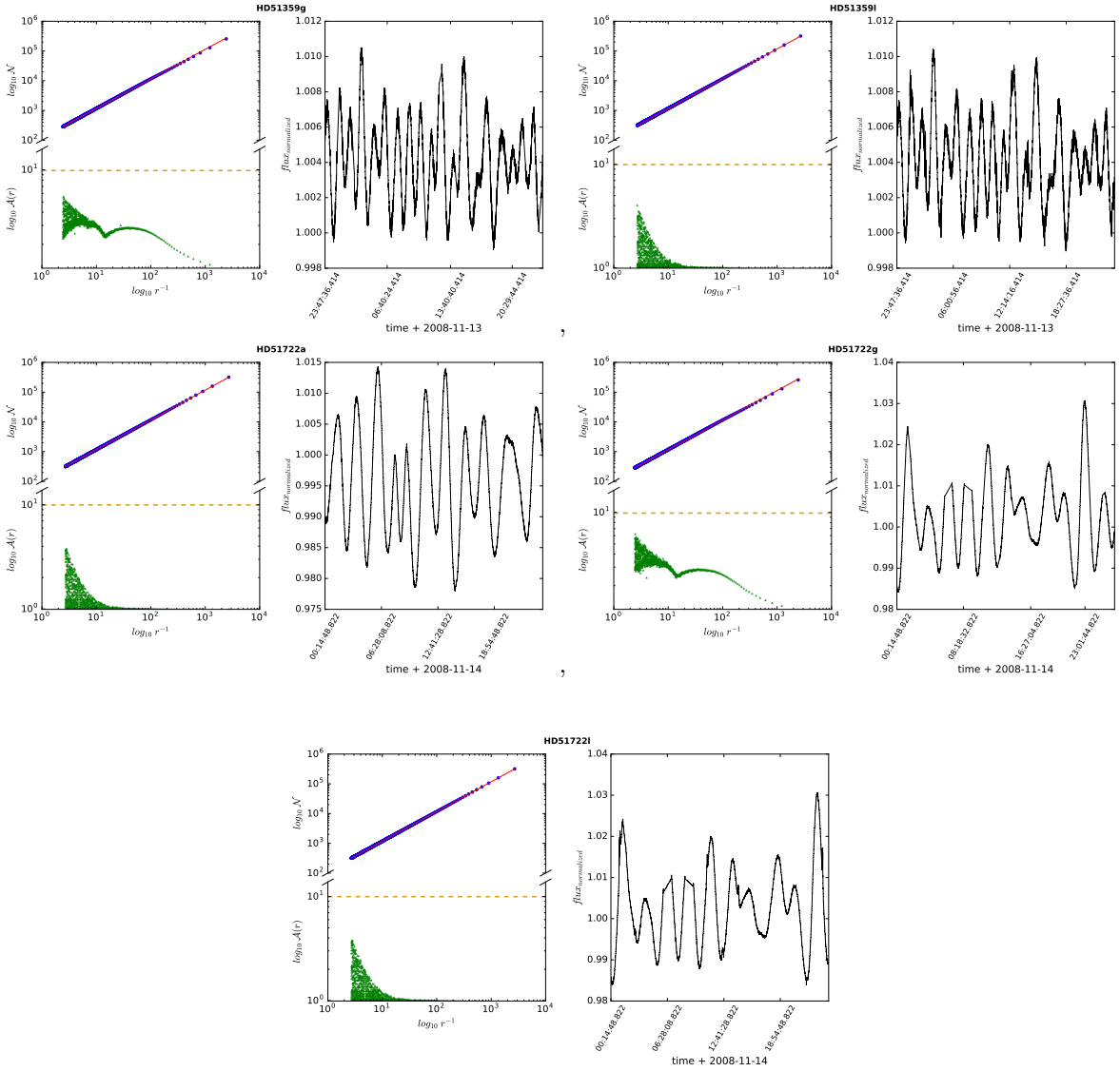

Figure 6: Set 6.